Heliyon 5 (2019) e02290

Contents lists available at ScienceDirect

Heliyon

journal homepage: www.heliyon.com

Pre-clinical anti-tumor activity of Bruton's Tyrosine Kinase inhibitor in Hodgkin's Lymphoma cellular and subcutaneous tumor model

Irfana Muqbil [a], Mahmoud Chaker [b], Amro Aboukameel [b], Ramzi M. Mohammad [b], Asfar S. Azmi [b], Radhakrishanan Ramchandren [c,*]

[a] Department of Chemistry, University of Detroit Mercy, Detroit, MI, USA
[b] Department of Oncology, Wayne State University School of Medicine, Karmanos Cancer Institute, Detroit, MI, USA
[c] Department of Medicine, University of Tennessee Knoxville, Knoxville Tennessee, USA

ARTICLE INFO

Keywords:
Cell biology
Molecular biology
Cancer research
Clinical toxicology
Oncology
Toxicology
Hodgkin's Lymphoma
Bruton's Tyrosine Kinase
Bruton's Tyrosine Kinase inhibitor
BTK
BTK inhibitor

ABSTRACT

Bruton's Tyrosine Kinase (BTK) is a member of the TEC family and plays a central role in B-cell signaling, activation, proliferation and differentiation. Here we evaluated the impact of BTK inhibitor Ibrutinib on a panel of HL models in vitro and in vivo. Ibrutinib suppressed viability and induced apoptosis in 4 HL cell lines in a dose and time dependent manner. Molecular analysis showed induction of both apoptotic and autophagy markers. Ibrutinib treatment resulted in suppression of BTK and other downstream targets including PI3K, mTOR and RICTOR. Ibrutinib given at 50 mg/kg p.o daily for three weeks caused statistically significant inhibition of HL cell line derived subcutaneous xenografts ($p < 0.01$) in ICR-SCID mice. Molecular analysis of residual tumor tissue revealed down-regulation of BTK; its related markers and autophagy markers. Our studies are the first showing in vitro and in vivo action of BTK inhibition in classical HL. A phase II study examining the activity of ibrutinib in relapsed or refractory HL is currently enrolling (NCT02824029).

1. Introduction

Hodgkin's Lymphoma (HL) is a malignancy of mature post germinal center B-lymphocytes that is diagnosed in approximately 9000 individuals annually in North America [1]. While the majority of patients diagnosed with HL are cured with multi-agent chemotherapy, a significant fraction of patients are refractory to conventional chemotherapy and almost half of patients with high-risk disease relapse [2]. HL is largely considered a malignancy of younger populations with a median age of diagnosis of 30 and is the most common malignancy of adolescence. For these patients few effective therapeutic options exist and the median survival is generally short. Importantly a second diagnostic peak occurs after age 55 and is associated with poorer outcomes. For these patients, conventional therapies may be associated with unacceptable toxicities. For patients who relapse after stem cell transplant or are not eligible for intensive therapy, the treatment is largely palliative with only three agents approved in the last 30 years for HL. Thus, novel molecularly driven therapies are critically needed to improve outcomes [3].

Bruton's Tyrosine Kinase (BTK) is a member of the TEC family [4] and plays a central role in B-cell signaling, activation, proliferation and differentiation [5]. Several studies have shown that BTK has been associated with common cancer associated pathways such as PI3K, mTOR, FAS and NF-κB [6]. Furthermore, BTK can be activated by IgM stimulation, CD40 ligand binding, chemokines and activation of toll like receptor (TLR) pathways [7]. Therefore, it is not surprising to note that BTK has been linked to the pathogenesis of various lymphomas [8]. These observations have given traction to strategies that target BTK inhibition and have ultimately enhanced the spectrum of therapeutic options in several B cell lymphomas including Mantle Cell Lymphoma (MCL), Chronic Lymphocytic Leukemia (CLL) and Waldenström's marcoglobulinemia [6].

The prognostic significance of BTK in HL has been established. Expression analysis of BTK in 395 different lymphomas and 14 malignant lymphoid cell lines compared to normal control showed more prominent expression in B cell lymphomas than in T cell lymphomas. More intriguingly, this study showed that among Hodgkin lymphomas, the nodular lymphocyte predominant variant was more often positive (>85%) than the classical variant (22%) [9]. In another study, analysis of the mutational landscape of HL has shown that in addition to classical alterations in pathways such as GM-CSF/IL-3, CBP/EP300, JAK/STAT,

* Corresponding author.
E-mail address: rramchandren@utmck.edu (R. Ramchandren).

https://doi.org/10.1016/j.heliyon.2019.e02290
Received 5 February 2019; Received in revised form 31 May 2019; Accepted 8 August 2019
2405-8440/© 2019 Published by Elsevier Ltd. This is an open access article under the CC BY-NC-ND license (http://creativecommons.org/licenses/by-nc-nd/4.0/).

NF-κB, there was also a prominent mutational load in numerous variants of genes affecting the B-cell receptor (BCR) pathway, such as *BTK*, *CARD11* and *BCL10* [10]. These independent findings suggest a possible mechanistic role for BTK in the pathobiology of HL and may therefore serve as a therapeutic target.

Ibrutinib is a first-in-class orally bioavailable small-molecule inhibitor of BTK. Ibrutinib covalently binds to the cys481 amino acid in the BTK active site [11]. This results in the blockade of adenosine triphosphate from binding and thus prevents activation of BTK by abrogation of its auto-phosphorylation. Due in part to the covalent nature of binding and having a short half-life, ibrutinib demonstrates high selectivity. This permits the use of a once daily dosing with a near-complete occupancy of the BTK active site in PBMCs. Although BTK is its primary target, Ibrutinib has also been shown to suppress interleukin-2–inducible T-cell kinase (ITK), tec protein tyrosine kinase (TEC), cytoplasmic tyrosine-protein kinase BMX, and epidermal growth factor receptor (EGFR) [5].

In spite of the observed alterations of BTK and its role in HL survival pathways, the impact of BTK targeted strategies using specific agents such as ibrutinib are yet to be explored. In this report we demonstrate the anti-proliferative effects of Ibrutinib in a series of HL cell lines with different genotypic and phenotypic makeup in vitro. To extend these studies and to model the characteristic clinical activity, we investigated the mechanism of action ibrutinib in subcutaneous mouse xenograft models derived from HL cells.

2. Materials and methods

The BTK inhibitor Ibrutinib (IB) was provided by Janssen (Janssen Medical Affairs Oncology, Janssen Services, LLC USA). A panel of HL cell lines [KM-H2 (Catalog # ACC-8 Hodgkin's Lymphoma representing mixed cellularity), L1236 (Catalog # ACC-530 Hodgkin's Lymphoma representing mixed cellularity), L-428 (Catalog # ACC-197 Hodgkin's Lymphoma representing nodular sclerosis)] and HDLM (lymphoid origin of Hodgkin and Reed-Sternberg cells) were obtained from DSMZ (Leibniz Institute DSMZ-German Collection of Microorganisms and Cell Cultures, Germany). Primary antibodies for BTK, PARP, Akt, pAkt, p65, Atg12, AC3B, Bcl-2, p53 and cleaved caspase 3 were purchased from Cell Signaling (Danver, MA USA). β-actin antibody and all secondary antibodies were obtained from Sigma (St. Louis, MO, USA).

2.1. Cell growth inhibition determined by the trypan blue assay

Cells were seeded at a density of 2×10^5 viable cells/mL in 24-well or 6-well culture plates (Costar, Cambridge, MA, USA), or 10-cm cell culture dishes (Corning Inc., Corning, NY, USA). All cells were maintained in RPMI 1640 medium supplemented with 10% fetal bovine serum (Hyclone Laboratories, Logan, UT, USA) and 1% penicillin-streptomycin (Invitrogen, Carlsbad, CA, USA), at 37 °C in a humidified incubator with 5% CO_2. The number of viable cells was determined by a trypan blue exclusion test [trypan blue (0.4%), Sigma Chemical Co. St. Louis, MO, USA]. Ibrutinib were added at indicated concentrations (0–20 μM) diluted from a 10 mM stock. The results were plotted as means ± SD of two separate experiments using three determinations per experiment for each experimental condition.

2.2. Quantification of apoptosis by Annexin V-FITC assay

Cell apoptosis was detected using an Annexin V-FITC assay (Biovision, Danvers, MA, USA) according to the manufacturers' protocols. HL cells were seeded at a density of 200,000 cells per well in six well plate in duplicate and treated with ibrutinib for 72 hrs. All procedures were performed according to our previously published protocols [12].

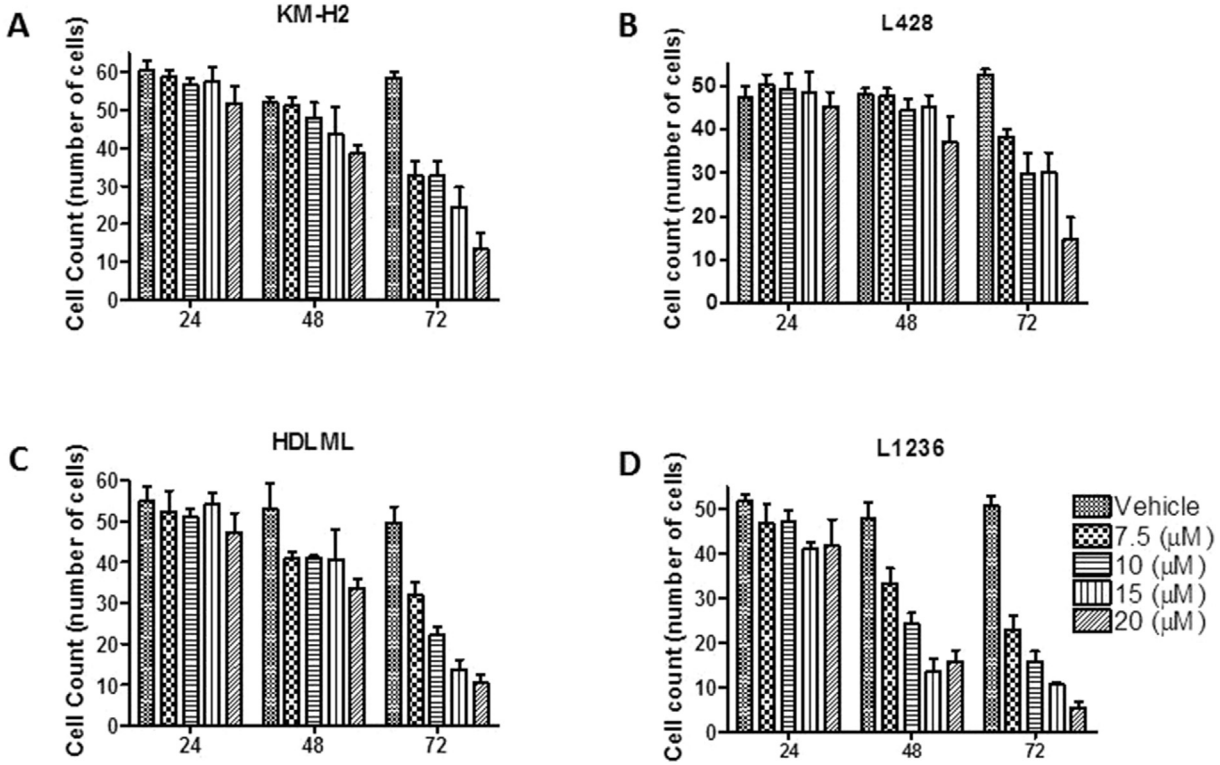

Fig. 1. Ibrutinib (BTK inhibitor) suppresses the activity of Hodgkin's Lymphoma cell lines. 4 different HL cell lines were seeded in 24 well plates at a density of 200,000 cells/well in triplicate and exposed to indicated concentrations of ibrutinib (BTK inhibitor) for 24–72 hrs. At the end of each treatment period cells were counted using Trypan Blue viability assessment method as described previously. Graph representative of two independent experiments [21].

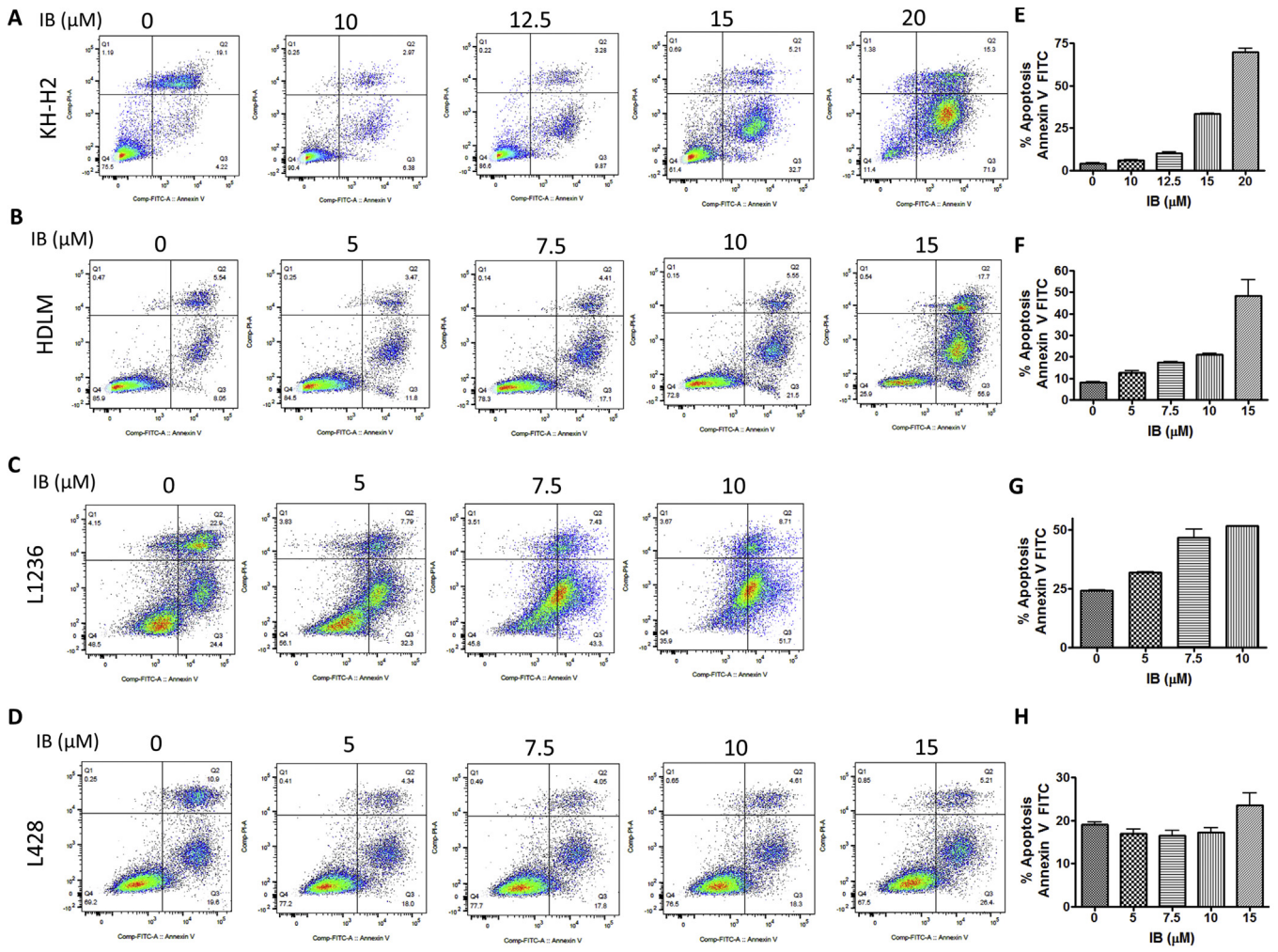

Fig. 2. Ibrutinib induces apoptosis in HL cell lines in a dose dependent manner. HL cells lines were grown in quadruplet in 24 well plates (200,000 cells per well) overnight. After 24 hrs the cells were exposed to indicated doses of ibrutinib for an additional 72 hrs. At the end of the treatment period, cells were centrifuged and re-suspended in 500 μL of Annexin binding buffer in Corning glass tubes. Each tube was mixed with 5 μL of Annexin and 5 μL of PI solution in dark and incubated for 5 minutes. The cells were sorted for apoptotic fraction using Becton Dickinson Flow cytometer at Karmanos Cancer Institute Flow cytometry core facility.

2.3. Western blot analysis

Cells (200,000) were grown in 24 well plates in triplicate and exposed to indicated concentrations of ibrutinib for 72 hrs. At the end of the treatment period, each treatment group was pooled followed by extraction of whole cell proteins for western blot analysis using previously described methods [13].

2.4. RT-PCR

Cells (200,000) were grown in 24 well plates in triplicate and exposed to indicated concentrations of ibrutinib for 72 hrs. At the end of treatment period, RNA was extracted according to standard published procedure [14]. Real-time RT-qPCR was conducted using High Capacity cDNA Reverse Transcription Kit and SYBR Green Master Mixture from Applied Biosystems (Waltham, MA). The PCR was initiated by 10 min at 95 °C before 40 thermal cycles, each of 15 s at 95 °C and 1 min at 60 °C on StepOnePlus system (Applied Biosystems). Data were analyzed according to the comparative Ct method and were normalized by actin and/or 18S rRNA expression in each sample. The primers used in this study were: BTK forward, 5′-aagcagttccttcaccgaga-3′; BTK reverse, 5′-ggacaggc cgaaatcagata-3′; RICTOR forward, 5′-ggtgttgtgactgaaacccg-3′; RICTOR reverse, 5′-gtcattccgccctcgtactc-3′; Akt forward, 5′-ttgtgaaggag ggttggctg-3′; Akt reverse, 5′-ctcacgttggtccacatcct-3′; PI3K forward 5′-gagccccgagcgtttctg-3′; PI3K reverse 5′-tcgtggaggcattgttctga-3′; 4EBP1 forward 5′-caagggatctgcccaccatt-3′; 4EBP1 reverse 5′-acac-gatggctggtgcttta-3′; ATG7 forward 5′-ttttggtcctagcagcccac-3′; ATG7 reverse 5′-tacggtcacggaagcaaaca-3′; ATG12 forward 5′-tgctggaggggaag-gactta-3′; ATG12 reverse 5′-gttcgctctactgcccactt-3′; Actin forward 5′- gca-cagagcctcgcctt-3′; Actin reverse 5′-tcatcatccatggtgagctg-3′; 18S forward 5′-gcaattattccccatgaacg-3′; 18S reverse 5′-ggcctcactaaaccatccaa-3′.

2.5. Development of animal xenograft and pre-clinical efficacy trial

Mouse xenograft was established as described previously [15]. The maximum tolerated dose (MTD) of ibrutinib in severe combined immunodeficient (ICR-SCID) mice was determined to be 50 mg/kg when given intravenously. Mice were treated with ibrutinib at doses of 50 mg/kg p.o 5 days a week for 4 weeks. Mice in the control and ibrutinib treated groups were followed for measurement of subcutaneous tumors, changes in body weight, and other side effects of the drugs. Tumors were measured twice weekly. Tumor weight (mg) was calculated using the formula: $(A \times B^2)/2$, where A and B are the tumor length and width (in mm), respectively. To avoid discomfort and in keeping with our Institutional Animal Care and Use Committee (IACUC) procedures, animals were euthanized when their total tumor burden reached 2,000 mg. All

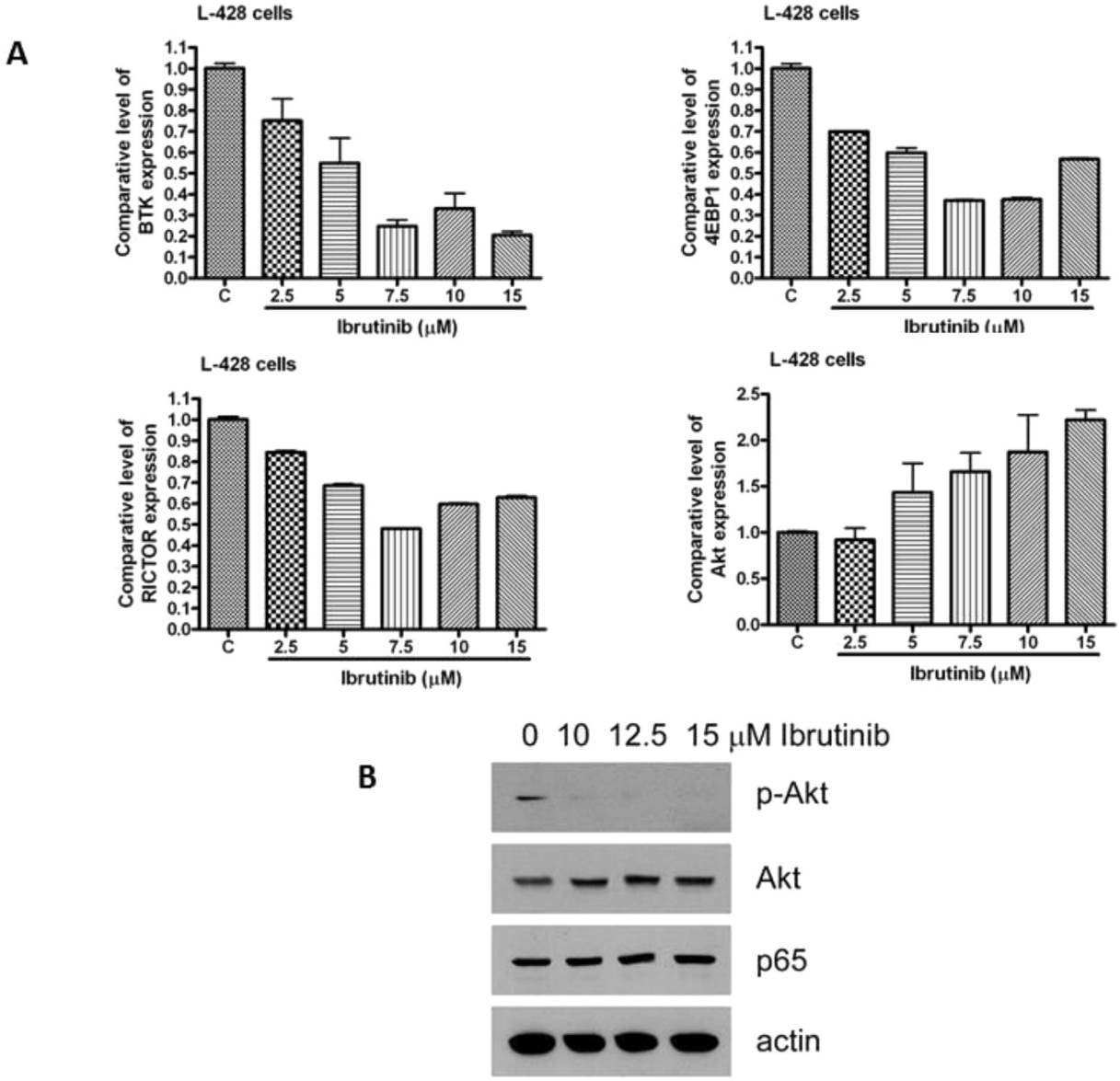

Fig. 3. Impact of Ibrutinib on downstream targets: L-428 cell lines were grown in 24 well plates at a density of 200,000 cells per well in quadruplet and exposed to indicated concentrations of Ibrutinib for 72 hrs. At the end of the treatment period cells were pooled and RNA was isolated and RT-PCR was performed using standard procedures (*$p < 0.05$; **$p < 0.01$). [B] KM-H2 cells were grown in 24 well plates in quadruplet and exposed to indicated concentrations of Ibrutinib for 72 hrs. At the end of the treatment the samples from individual treatment groups were pooled and protein was isolated using standard procedures. The proteins lysates were resolved using polyacrylamide gel electrophoresis and Western Blotting. The blots were probed for antibodies against BTK, pAkt and p65. β-actin was used as a loading control. Original uncropped gel images can be viewed in Supplementary Fig. 1.

studies involving mice were done under Animal Investigation Committee-approved protocols. Residual tissue from the control and treatment groups was analyzed for changes in molecular markers by western blotting and RT-PCR by standard procedures.

2.6. Statistical analysis

Wherever appropriate, the data were subjected to a Student's t-test using GraphPad Prism software (La Jolla, CA). $p < 0.05$ was considered statistically significant.

3. Results

3.1. Ibrutinib prevents HL proliferation

In order to evaluate the cell proliferation inhibition potential, classical HL cell lines (KM-H2, L1236, L-428 and HDLML) were exposed to Ibrutinib (0–25 micro M concentrations for 0–72 hrs) followed by trypan blue viability analysis. As can be seen from the results of Fig. 1 (A–D), exposure to Ibrutinib resulted in marked suppression of HL cell lines in a time and dose dependent manner. All the cells lines tested demonstrated response to ibrutinib with a IC_{50} in the range of 7.5–10 μM. These results for the first time show that Ibrutinib is effective in suppressing the proliferation of HL cells and support its credentials to be used as a new therapy for this disease.

3.2. Ibrutinib induced apoptosis in HL cells

To verify whether the cell death proliferation inhibition by Ibrutinib was consistent with apoptosis induction, Annexin V FITC assay was performed. As can be seen from the results of Fig. 2, Ibrutinib treatment resulted in statistically significant induction of apoptosis in KM-H2

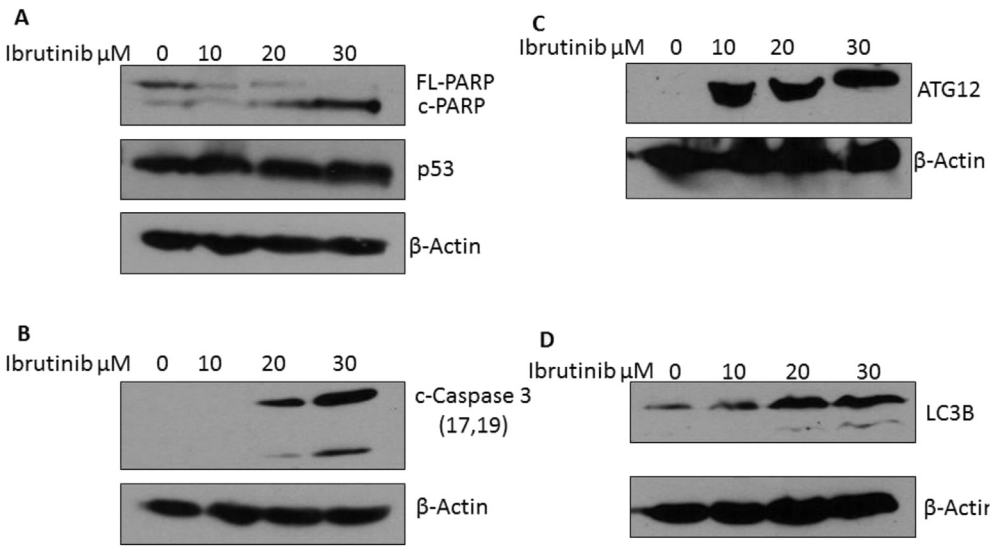

Fig. 4. Protein expression analysis post ibrutinib treatment. L-428 cell lines were grown in T75 culture flask in the presence of indicated doses of Ibrutinib for 72 hrs. At the end of the treatment period cells protein was isolated and western blot was performed using standard protocols [22]. Blots were probed for antibodies against PARP, cleaved Caspase 3, ATG12 and LC3B (see methods for antibody source). β-actin was used as a loading control. Blots are representative of two independent experiments. Original uncropped gel images can be viewed in Supplementary Figs. 2–5.

(Fig. 2A ~4% apoptosis in control vs ~33% apoptosis at 10 μM and ~70% apoptosis at 20 μM ibrutinib); L1236 (Fig. 2B); L428 (Fig. 2C) and HDLM (~8% apoptosis in control vs ~50% apoptosis at 15 μM). In agreement with the viability assay findings, apoptosis was consistently observed in all the cell lines indicating that the drug could impact HL irrespective of the sub-types of the disease.

3.3. Molecular analysis of ibrutinib targeted pathways in HL

In order to evaluate the signaling mechanisms regulated by ibrutinib in HL cells RT-PCR and western blotting was performed. As can be seen from the results of Fig. 3A, treatment of HL cells ibrutinib (to IC_{50} or related doses) resulted in statistically significant down-regulation in the mRNA levels of the drug's primary target BTK in L428 cells in a dose dependent manner. Additionally, we also observed down-regulation of BTK downstream effectors 4EBP1 and RICTOR. Total AKT levels showed only a slight increase that was not significant at the mRNA level. Following this we also analyzed the protein expression changes in BTK regulated proteins post ibrutinib treatment. As can be seen from the results of Fig. 3B, ibrutinib treatment resulted in significant down-regulation phospho-Akt levels. The levels of total Akt and NF-κB complex component p65 did not decrease significantly. These results indicate that ibrutinib treatment modulates the targets downstream effectors in HL.

3.4. Ibrutinib activates autophagy pathways in HL cells

Despite prominent apoptotic cell death observed in the 4 different cell lines tested, we did not observe significant changes in some of the classical pro-apoptotic markers. A limited set of proteins from the apoptosis cascade such as cleavage of PARP and caspase 3 were observed post ibrutinib treatment (Fig. 4A and B). Similarly there was no significant change in p53 expression (Fig. 4A middle lane). Therefore, in order to enhance our understanding of the cytotoxic mechanisms of ibrutinib we expanded our molecular analysis and evaluated non-classical cell death marker proteins. Interestingly, probing for autophagy markers revealed a unique mechanism of ibrutinib cell death induction in these cells. As can be seen from the results of Fig. 4 C and D, we observed enhancement in the expression of well-known autophagy markers LC3B, and ATG12. These results clearly show that ibrutinib mediated cell death in HL goes well beyond the classical apoptosis pathway and that additional anti-proliferative pathways are activated by the drug.

3.5. Pre-clinical anti-tumor efficacy trial of ibrutinib in HL sub-cutaneous xenograft

Next we probed for the in vivo anti-tumor activity of ibrutinib in KM-H2 subcutaneous xenografts. Oral treatment of ibrutinib (50 mg/kg p.o once daily 5 days a week for 4 weeks) to mice harboring KM-H2 at the sub-cutaneous site ($n = 5$) resulted in statistically significant reduction of tumor growth ($P < 0.001$) (Fig. 5A graph showing tumor weight, Fig. 5B gross tumor weight 24 hrs post last drug dosing and Fig. 5C excised tumor images post treatment). Ibrutinib was found to be tolerated at this dose with no outward body weight loss (<10%) and no discomfort to animals. RNA from excised residuals tumors was subjected to RT-PCR analysis to capture molecular markers. As can be seen from the results of Fig. 5E and results that are aligned to our *in vitro* observations, ibrutinib treatment resulted in marked reduction of mRNA levels of BTK, 4EBP1, RICTOR and PI3K in the residual HL tumors. We also observed activation of autophagy markers in the residual tumors (LC3A, LC3B, ATG12 and Beclin 5E Lower panel). These findings were consistent with those noted in cell lines indicating that the postulated mechanisms of action of ibrutinib in HL may be translated to in vivo models.

4. Discussion

In this report we for the first time demonstrate the activity of Bruton's Tyrosine Kinase inhibitor ibrutinib in classical Hodgkin's Lymphoma (HL) models *in vitro* and in *in vivo*. Mechanistically we show that ibrutinib induces several cell death mechanisms (apoptosis and autophagy) in HL and support the utility of BTK as a therapeutic target for this disease. Based on this work a phase II study examining the activity of ibrutinib in relapsed or refractory HL is currently enrolling (NCT02824029). Importantly, presentations from this study and case reports of therapeutic response to ibrutinib have been presented or published indicating the potential clinical activity of this agent in HL.

Each year over 8000 Americans are diagnosed with HL and ~1000 die from this disease [16]. Despite some success with available radiotherapy and systemic chemotherapies, there is a need for the development of novel molecular targeted strategies that have minimal long term toxcities [17]. Notably, ibrutinib treatment resulted in the suppression of the proliferative potential of several distinct HL cell lines. Although these IC50s are higher than clinically achieved concentrations of ibrutinib, these are consistent with reported in vitro activity in chronic lymphocytic leukemia (CLL) and other lymphomas where ibrutinib is clinically active, perhaps reflecting that the physiological microenvironment may also play a role [18]. Nonetheless, inhibition of proliferation is observed in

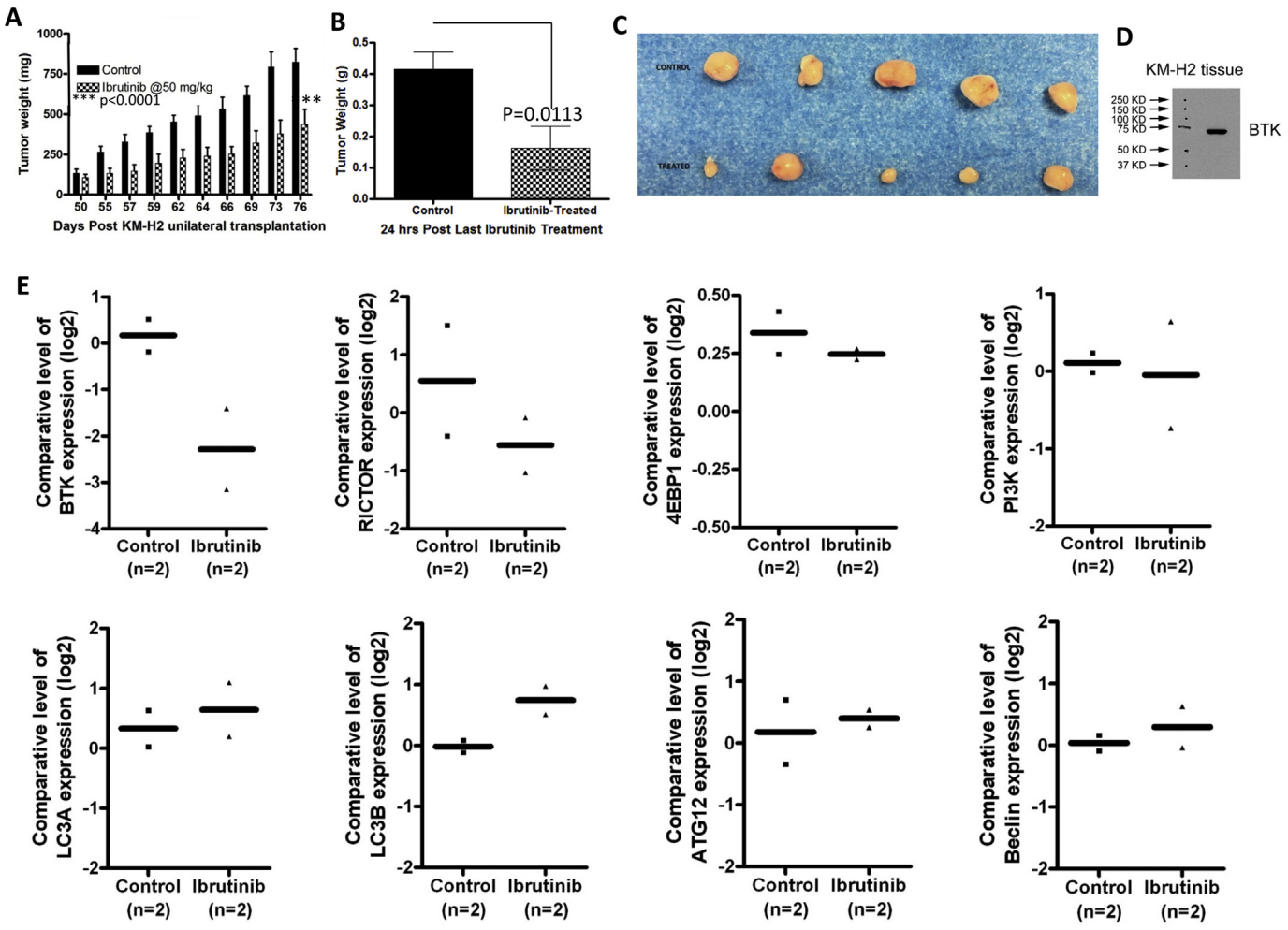

Fig. 5. Ibrutinib suppresses the growth of KM-H2 subcutaneous xenograft in a statistically significant manner. Initially, $5X10^6$ KM-H2 100% viable cells were subcutaneously injected bilaterally in 5–6 ICR-SCID mice. After several attempts, and once tumor(s) develop, they were surgically removed, dissected into ~100 mg tumor pieces, and transplanted into the flanks of 15 naïve, 4-5-week-old female ICR-SCID mice. Roughly two months later, 10 mice that developed sizable tumors were randomly divided into two equal cohorts; Control (received diluent) and Ibrutinib-treated (orally 50 mg/kg qd X5 X3–4 weeks). [A] Graph showing anti-tumor efficacy. [B] Gross tumor weight at the last dose treatment. [C] Images of tumors excised from mice after treatment. [D] One mice was sacrificed to check the expression of BTK and one mice was sacrificed to check the tumor quality. (Tumor weight calculated by vernier caliper by multiplying the length by $width^2/2$) as described previously [23]. Molecular analysis of residual tumor tissue using RT-PCR. Total RNAs from 2 tumor tissues were extracted by using the RNeasy Mini Kit (QIAGEN, Valencia, CA) following the protocol provided by the manufacturer. The RNA (1μg) from each sample was converted to cDNA by using High Capacity cDNA Reverse Transcription Kit (Applied Biosystems, Foster City, CA). The expression level of BTK, PI3K, Akt, RICTOR, and 4EBP1 in cells or tumors was analyzed by real-time qPCR using SYBR Green Master Mixture from Applied Biosystems. Data was analyzed according to the comparative Ct method and was normalized by GAPDH and 18S rRNA expression in each sample. Original uncropped gel images can be viewed in Supplementary Fig. 6.

vitro and was concurrent with induction of both apoptotic type cell death (Annexin V positivity) and autophagy. We observed significant down-regulation of BTK and its related downstream markers. Notably, probing for molecular changes showed that ibrutinib treatment caused an autophagic cell death in HL cells in addition to classical apoptotic pathway activations. (PARP and caspase cleavage concurrent with significant activation of autophagy markers Beclin, ATG12, LC13B). These results are strongly supported by the in vivo results from the KM-H2 mouse xenograft model, in which ibrutinib significantly inhibits tumor growth compared to control. Downregulation of BTK and downstream effectors as well as upregulation of autophagic markers are also observed these tumors, akin to the in vitro results. Notably, the in vivo data show persistence of remaining tumor even after 72 days of ibrutinib treatment, suggesting that ibrutinib alone may provide tumor growth control but that combination with other apoptosis-inducing agents may be needed for tumor eradication. Supporting these studies in a glioblastoma model, Wang and colleagues showed that anti-tumor mechanism of action of ibrutinib involved activation of autophagy pathways [19]. In another study in skin cancer model, ibrutinib was shown to induce cell death through the activation of autophagy [20]. These findings suggest that ibrutinib may have meaningful biologic activity beyond BTK/BCR/NF-kB pathway inhibition alone and may induce tumor death through multiple mechanisms.

In conclusion the present studies demonstrate the potential utility of targeting BTK with ibrutinib in HL and provide further insights into the mechanisms of ibrutinib-mediated tumor grown inhibition and tumor death, which may guide further studies of ibrutinib in the future.

Declarations

Author contribution statement

Irfana Muqbil, Mahmoud Chaker, Amro Aboukameel: Performed the experiments; Analyzed and interpreted the data; Contributed reagents,

materials, analysis tools or data and wrote the paper.

Ramzi M. Mohammad: Conceived and designed the experiments; Analyzed and interpreted the data; Contributed reagents, materials, analysis tools or data and wrote the paper.

Asfar S. Azmi: Conceived and designed the experiments; Performed the experiments; Analyzed and interpreted the data; Contributed reagents, materials, analysis tools or data and wrote the paper.

Radhakrishanan Ramchandren: Conceived and designed the experiments; Contributed reagents, materials, analysis tools or data and wrote the paper.

Funding statement

This work was supported by Jannssen LLC.

Competing interest statement

The authors declare the following conflict of interests: Radhakrishanan Ramchandren and Asfar S. Azmi received funding fron Jannsen LLC to conduct this study. All other authors have no conflict of interest.

Additional information

Supplementary content related to this article has been published online at https://doi.org/10.1016/j.heliyon.2019.e02290.

References

[1] A. Mottok, C. Steidl, Biology of classical Hodgkin lymphoma: implications for prognosis and novel therapies, Blood (2018).
[2] A. Kallam, J.O. Armitage, Current and emerging treatment options for a patient with a second relapse of Hodgkin's lymphoma, Expert Rev. Hematol. 11 (2018) 293–300.
[3] N.L. Bartlett, Emerging role of novel therapies in Hodgkin lymphoma: proceed with caution, Hematology. Am. Soc. Hematol. Educ. Program. 2017 (2017) 317–323.
[4] Y. Qiu, H.J. Kung, Signaling network of the Btk family kinases, Oncogene 19 (2000) 5651–5661.
[5] S.S. Pal, F. Dammeijer, R.W. Hendriks, Role of Bruton's tyrosine kinase in B cells and malignancies, Mol. Cancer 17 (2018) 57.
[6] T. Seiler, M. Dreyling, Bruton's tyrosine kinase inhibitors in B-cell lymphoma: current experience and future perspectives, Expert Opin. Investig. Drugs 26 (2017) 909–915.
[7] C. Brunner, A. Avots, H.W. Kreth, E. Serfling, V. Schuster, Bruton's tyrosine kinase is activated upon CD40 stimulation in human B lymphocytes, Immunobiology 206 (2002) 432–440.
[8] C.U. Niemann, A. Wiestner, B-cell receptor signaling as a driver of lymphoma development and evolution, Semin. Cancer Biol. 23 (2013) 410–421.
[9] I. Fernandez-Vega, L.M. Quiros, J. Santos-Juanes, M. Pane-Foix, T. Marafioti, Bruton's tyrosine kinase (Btk) is a useful marker for Hodgkin and B cell non-Hodgkin lymphoma, Virchows Arch. 466 (2015) 229–235.
[10] E. Mata, A. Diaz-Lopez, A.M. Martin-Moreno, M. Sanchez-Beato, I. Varela, M.J. Mestre, C. Santonja, F. Burgos, J. Menarguez, M. Estevez, M. Provencio, B. Sanchez-Espiridion, E. Diaz, C. Montalban, M.A. Piris, J.F. Garcia, Analysis of the mutational landscape of classic Hodgkin lymphoma identifies disease heterogeneity and potential therapeutic targets, Oncotarget 8 (2017) 111386–111395.
[11] A. Hamasy, Q. Wang, K.E. Blomberg, D.K. Mohammad, L. Yu, M. Vihinen, A. Berglof, C.I. Smith, Substitution scanning identifies a novel, catalytically active ibrutinib-resistant BTK cysteine 481 to threonine (C481T) variant, Leukemia 31 (2017) 177–185.
[12] A.S. Azmi, A. Al-Katib, A. Aboukameel, D. McCauley, M. Kauffman, S. Shacham, R.M. Mohammad, Selective inhibitors of nuclear export for the treatment of non-Hodgkin's lymphomas, Haematologica 98 (2013) 1098–1106.
[13] A.M. Sosin, A.M. Burger, A. Siddiqi, J. Abrams, R.M. Mohammad, A.M. Al-Katib, HDM2 antagonist MI-219 (spiro-oxindole), but not Nutlin-3 (cis-imidazoline), regulates p53 through enhanced HDM2 autoubiquitination and degradation in human malignant B-cell lymphomas, J. Hematol. Oncol. 5 (2012) 57.
[14] A.S. Azmi, I. Muqbil, J. Wu, A. Aboukameel, W. Senapedis, E. Baloglu, A. Bollig-Fischer, G. Dyson, M. Kauffman, Y. Landesman, S. Shacham, P.A. Philip, R.M. Mohammad, Targeting the nuclear export protein XPO1/CRM1 reverses epithelial to mesenchymal transition, Sci. Rep. 5 (2015) 16077.
[15] R.M. Mohammad, N.R. Wall, J.A. Dutcher, A.M. Al-Katib, The addition of bryostatin 1 to cyclophosphamide, doxorubicin, vincristine, and prednisone (CHOP) chemotherapy improves response in a CHOP-resistant human diffuse large cell lymphoma xenograft model, Clin. Cancer Res. 6 (2000) 4950–4956.
[16] R.L. Siegel, K.D. Miller, A. Jemal, Cancer statistics, 2018, CA Cancer J. Clin. 68 (2018) 7–30.
[17] B. Rathore, M.E. Kadin, Hodgkin's lymphoma therapy: past, present, and future, Expert Opin. Pharmacother. 11 (2010) 2891–2906.
[18] A. Rosenthal, Small molecule inhibitors in chronic lymphocytic lymphoma and B cell non-Hodgkin lymphoma, Curr. Hematol. Malig. Rep. 12 (2017) 207–216.
[19] J. Wang, X. Liu, Y. Hong, S. Wang, P. Chen, A. Gu, X. Guo, P. Zhao, Ibrutinib, a Bruton's tyrosine kinase inhibitor, exhibits antitumoral activity and induces autophagy in glioblastoma, J. Exp. Clin. Cancer Res. 36 (2017) 96.
[20] F.D. Sun, P.C. Wang, J. Shang, S.H. Zou, X. Du, Ibrutinib presents antitumor activity in skin cancer and induces autophagy, Eur. Rev. Med. Pharmacol. Sci. 22 (2018) 561–566.
[21] I. Muqbil, A. Aboukameel, S. Elloul, R. Carlson, W. Senapedis, E. Baloglu, M. Kauffman, S. Shacham, D. Bhutani, J. Zonder, A.S. Azmi, R.M. Mohammad, Anti-tumor activity of selective inhibitor of nuclear export (SINE) compounds, is enhanced in non-Hodgkin lymphoma through combination with mTOR inhibitor and dexamethasone, Cancer Lett. 383 (2016) 309–317.
[22] A.S. Azmi, Y. Li, I. Muqbil, A. Aboukameel, W. Senapedis, E. Baloglu, Y. Landesman, S. Shacham, M.G. Kauffman, P.A. Philip, R.M. Mohammad, Exportin 1 (XPO1) inhibition leads to restoration of tumor suppressor miR-145 and consequent suppression of pancreatic cancer cell proliferation and migration, Oncotarget 8 (2017) 82144–82155.
[23] R.M. Mohammad, S. Wang, A. Aboukameel, B. Chen, X. Wu, J. Chen, A. Al-Katib, Preclinical studies of a nonpeptidic small-molecule inhibitor of Bcl-2 and Bcl-X(L) [(-)-gossypol] against diffuse large cell lymphoma, Mol. Cancer Ther. 4 (2005) 13–21.